Proceedings of the 34th Chinese Control Conference
July 28-30, 2015, Hangzhou, China

Localizing Multiple Odor Sources with a Mobile Robot in Time-varying Airflow Environments using Dempster-Shafer Inference

LI Ji-Gong[1,2], ZHOU Jie-Yong[1,2], YANG Jing[3], LIU Jia[1,2], ZENG Fan-Lin[1,2], YANG Li[1,2]

1. School of Automation and Electrical Engineering, Tianjin University of Technology and Education, Tianjin 300222, China

2. Tianjin Key Laboratory of Information Sensing and Intelligent Control, Tianjin 300222, China

E-mail: charles75@163.com

3. School of Information Technology Engineering, Tianjin University of Technology and Education, Tianjin, 300222, China

E-mail: tracy_7904@163.com

Abstract: This paper addresses the problem of multiple odor sources localization (MOSL) using a mobile robot in a time-varying airflow environment, and provides a localization method which applies the Dempster-Shafer (D-S) theory to map the possible locations of several odor sources and then uses the map to plan a searching route online for the robot. In the proposed method, the robot carries out the D-S inference and iteratively updates a grid map in which each cell has two states (i.e., occupied by an odor source, and not occupied by odor source), using the successive measurements from a gas sensor and an anemometer when the robot follows the dynamic-planned searching route in the given work area. The searching route is planned online to maximize the decline of the uncertainties of the grid cells around the robot. The mapping of the odor sources and the planning of the searching route work side-by-side. Simulations are carried out and the results in a time-varying airflow environment show that the locations of the two odor sources can be estimated online with the D-S inference, and the time cost can be greatly reduced by following the dynamic-planned searching route compared with by following a predefined path shaped like rectangular wave to cover the given searching area.

Key Words: Multiple odor sources localization, mobile robot, D-S inference, online estimating and searching

1 Introduction

Odor information is widely used by many animals for searching for food, finding mates, exchanging information, and evading predators. Inspired by the olfaction abilities of many animals, in the early 1990s, people started to try building mobile robots with similar olfaction abilities to replace trained animals [1-4]. Compared to animals, robots can be deployed quickly and maintained with low cost. In addition, robots can work for long periods without fatigue, and most importantly, they can enter dangerous areas. It is expected that mobile robots developed with such olfaction capability will play more and more roles in such areas as judging toxic or harmful gas leakage location, checking for contraband (e.g., heroin), searching for survivors in collapsed buildings, humanitarian de-mining, and antiterrorist attacks.

The methods of odor source localization (OSL) realized using an individual or multiple mobile robots can be classified into tracing-behavior-based methods and analytical-model-based methods [5]. In the tracing-behavior-based group, the source location is often determined by the final position of the mobile robot doing plume tracing and successfully arriving at the source. An alternate name for OSL, chemical plume tracing [6, 7], reflects the importance of the plume-tracing strategy in these methods. Some biologically inspired approaches have been designed for mobile robot based plume tracing, such as gradient-following-based algorithm in low Reynolds number [8] and up-wind algorithm in a wind tunnel [9], which intended to mimic the behaviors of chemotaxis and anemotaxis of a few biological entities, respectively. However, the airflow in practical environments is almost always turbulent with a relative high Reynolds number, which results in intermittent and time-varying plumes. In addition, an odor source is not necessarily in up-wind direction due to the meander of plumes in time-varying flow fields. Moreover, some engineered plume tracing strategies have also been proposed, such as fluxotaxis [7] and infotaxis [10] algorithms. The fluxotaxis method is a multi-robot based approach, in which the knowledge of computational fluid dynamics is applied. The infotaxis uses the information entropy to guide robot searching for an odor source, but only simulation results were provided in [10]. In addition, a combination of the biomimetic and engineered strategies can be found in [11].

For tracing-behavior-based methods, it is difficult for the robot to automatically provide the source location with its final position because the robot cannot know whether it arrives at the source. Therefore, to automatically obtain the source location by the robot itself, an analytical-model-based method is necessary.

Comparatively, only a few analytical-model-based methods have been reported, such as modeling the wind field using naive physics [12, 13], remote gas source localization [14], building gas distribution grid maps [15], a source-likelihood mapping approach based on the Bayesian inference method [16], mapping multiple odor sources using

* This work is supported by Tianjin Natural Science Foundation under Grant 13JCYBJC17500, the National Natural Science Foundation of China (No. 61304153), the Science and Technology Development Foundation of Tianjin Higher Education under Grant 20120808 and 20120828, and the Scientific Research Foundation of Tianjin University of Technology and Education under Grant KYQD14012 and KJY1302.

Bayesian occupancy grid map [17], and localizing via Particle Filter [18] in our earlier work, etc. However, the methods proposed in [12-15] and [17] might not work in real outdoor environments because the required conditions, i.e., stable airflow field or weak airflow, are hardly satisfied in outdoor environments where the airflow is almost always turbulent, time varying, and strong. And the methods presented in [16] and [18] only suit the cases with a single odor source. Unfortunately, large amount of OSL problems not only happen in environments with turbulent flow, but also likely involve multiple odor sources.

In our most recent work [19], a multiple-odor-sources localization (MOSL) method via D-S inference was proposed to map the locations of the odor sources while the robot follows a predefined path shaped like rectangular wave to cover the given searching region in an outdoor environment with time-varying airflow. Due to the significant variation of the airflow in outdoor environments, especially in direction, the searching area always can not be checked evenly although the robot explores the region evenly by following the rectangular-wave-shaped path. In addition, the robot has to spend much time to cover the searching area several rounds, and the efficiency of the work seems not high.

In order to improve the performance of the MOSL using D-S inference, this paper presents an efficient solution in which the real-time result of odor-sources mapping is used to guide the exploration of the robot. The exploratory behavior of the robot is to follow a dynamic-planned route rather than the predefined path shaped like rectangular wave in our previous work [19] to cover the given searching region. The searching route is planned in real time according to the current result of the odor-sources mapping and the measurements of the wind to maximize the decline of the uncertainties of the grid cells around the robot. The mapping of the odor sources and the planning of the searching route work side-by-side.

The remainder of this paper is organized as follows. Section 2 reviews the D-S inference for MOSL in [19]. The path planning for exploration is described in section 3. The simulation, comparison and the conclusion are presented in the rest of the paper.

2 D-S Inference for MOSL

Consider Θ to represent all possible states of the frame of discernment and the power set 2^{Θ} to represent the set of all possible subsets of Θ. In contrast to probability theory that assigns a probability mass to each element of Θ, D–S theory assigns belief mass m to each element e of 2^{Θ}, which represent possible propositions regarding the system state. Function m has two properties: $m(\phi)=0$ and $\sum_{e\in 2^{\Theta}} m(e)=1$.

2.1 MOSL using D-S Inference

The distribution of the odor sources can be conveniently represented by a grid map $\{C_i, i=1,2,\cdots M\}$ since the odor sources are immovable in most OSL applications, where the constant M is the number of the cells in the grid map. For each cell C_i in the grid map, it has two states, named S (occupied by an odor source), $\overline{S}$ (not occupied by odor source), respectively, composing a frame of discernment $\Theta=\{S,\overline{S}\}$.

Intuitively for any proposition e, $m(e)$ represents the proportion of available evidence that supports the claim that the actual cell state belongs to e. When the robot takes a measurement, there will be a piece of evidence. Given two pieces of evidence with corresponding belief mass functions $m_1(e_1)$ and $m_2(e_2)$, $e_1, e_2 \in 2^{\Theta}$ (to be detailed in section 2.2), using the Dempster's rule of combination, the two pieces of evidence can be fused and produce a joint belief mass function $m_{1,2}(e)$ as [20]

$$m_{1,2}(e)=(m_1\oplus m_2)(e)=\sum_{e_1\cap e_2=e\neq\phi} m_1(e_1)m_2(e_2)/(1-K), \quad (1)$$

where K represents the amount of conflict between the two evidences and is given by

$$K=\sum_{e_1\cap e_2=\phi} m_1(e_1)m_2(e_2). \quad (2)$$

It is not hard to find that the power set 2^{Θ} only has four elements, ϕ, $\{S\}$, $\{\overline{S}\}$, and $\{S,\overline{S}\}$ (i.e., Θ). In order to understand easily, here we denote the subset $\{S,\overline{S}\}$ as U (unknown). Thus, there is

$$m(S)+m(\overline{S})+m(U)=1. \quad (3)$$

Since the frame of discernment $\Theta=\{S,\overline{S}\}$ only has two states, the proposed D-S inference for MOSL itself is simple and will not suffer the exponential complexity of computations. In addition, because the Dempster's rule of combination satisfies the associative law, i.e., $m_1\oplus m_2\oplus m_3=(m_1\oplus m_2)\oplus m_3=m_1\oplus(m_2\oplus m_3)$, thus there is $m_1\oplus m_2\oplus\cdots\oplus m_n=(m_1\oplus m_2\oplus\cdots\oplus m_{n-1})\oplus m_n$, therefore we can easily perform a recursively inference using new coming evidence from the successive measurements by the robot.

2.2 Belief Mass Function for MOSL

It is well known that the odor dispersion is dominated by the turbulent dispersion, the odor molecules are transported by environmental fluid such as air. If we regard air as a body consisting of many air masses (such as eddies on the order of the odor puff size in physics), then not only are there air masses containing enough odor molecules, but also air masses without enough odor molecules or even having no odor molecule. When robot encounters the former, an odor detection event would be happen, the latter a non-detection event. Because both the detection and non-detection events will be helpful to localize the odor source, so we use an item "air-mass path" which is defined as the trajectory most likely taken by an air mass encountered with the mobile robot.

We can get an estimation of air-mass path [19]. Intuitively,

if we get a detection event, the area covered by the estimated air-mass path will likely contain one or some odor sources. Otherwise, the possibility there are some odor sources in the covered region will decrease.

Let the set $\{\pi_i, i = 1,2,\cdots M\}$ denote the probability map of the air-mass path, where the constant M is the number of the cells in the grid map, and π_i indicates the probability that the air mass arrived at the robot comes from the cell C_i. π_i can be calculated with the algorithm specified in [19]. Therefore, the belief mass function can be given for both detection event D and non-detection event $\overline{D}$ respectively as follows:

$$m(e)|_i^D = \begin{cases} \mu_D \zeta \pi_i & e = S \\ 0 & e = \overline{S} \\ 1 - \mu_D \zeta \pi_i & e = U \end{cases}, \quad \text{(4-a)}$$

$$m(e)|_i^{\overline{D}} = \begin{cases} 0 & e = S \\ \mu_{\overline{D}} \zeta \rho \pi_i & e = \overline{S} \\ 1 - \mu_{\overline{D}} \zeta \rho \pi_i & e = U \end{cases}, \quad \text{(4-b)}$$

where μ_D is the probability of detection event D arising given that there is detectable odor at the position of the robot; $\mu_{\overline{D}}$ is the probability of non-detection event $\overline{D}$ happening given that there is no detectable odor at the position of the robot; ζ represents the reliability of the model of the air mass transportation; ρ indicates the reliability decreasing because of the intermittency of the odor plume or the lack of enough odor molecules (easily cause the false non-detection event).

According to our test data of the gas sensor, $\mu_D \approx 0.9$, $\mu_{\overline{D}} \approx 1.0$; ζ and ρ vary with the distance from a location to the robot, and we conservatively choose $\zeta \approx 0.6$ and $\rho = 0.5$ in this research.

3 Path Planning for Exploration

The searching path concerned in this section is planned in real time, and works side-by-side with the mapping of the odor sources detailed in section 2. In order to improve the efficiency of the exploration, the searching route should be planned online to maximize the decline of the uncertainties of the grid cells, making the cells' states clear whether the cells are occupied by an odor source or not occupied by odor source. Before the searching path planning is described, the uncertainty X_i of a grid cell C_i should be defined first as follows.

$$X_i = -[m(S)\log 2^{m(S)} + m(\overline{S})\log 2^{m(\overline{S})}] + qm(U), \quad (5)$$

where the first item $-[m(S)\log 2^{m(S)} + m(\overline{S})\log 2^{m(\overline{S})}]$ is the information entropy about the two states S and $\overline{S}$ of the cell C_i, and q is a constant indicating the weight of the unknown state in the total uncertainty X_i, and is chosen as 3.0 in current research. Apparently, the larger the uncertainty X_i, the less information is known about the cell, and more searching should be carried out for the cell. As the searching goes on, the uncertainty X_i would decrease in general and eventually converge to zero. X_i becomes zero means the state of the cell is definitely clear, whether the cell is in state S or $\overline{S}$, and it is unnecessary to perform more exploration for the cell.

To find out where the robot should to go to maximize the decline of the uncertainties of the grid cells, a number of positions around the robot are evaluated with the following criterion,

$$E_P = \sum_{i=1}^{M} \pi_i^{P*} X_i, \quad (6)$$

where E_P is defined as the fitness that the robot went to the position P, π_i^{P*} represents the probability that the air mass which would arrive at P at the next time step comes from the cell C_i. The larger the value of E_P, the more uncertainties of the cells in the estimated air-mass path $\{\pi_i^{P*}, i = 1,2,\cdots M\}$ would be decreased if the robot went to position P in the next time step.

Since π_i^{P*} is hard to estimate, we have to approximate π_i^{P*} with $\pi_{i+\Delta}$ on the uniform assumption of the airflow field [18] and regardless a time-step difference, where Δ is the offset from the current location of the robot to the position P. For convenience, the position P is selected as the center of a grid cell. Thus we have

$$E_P \approx \sum_{i=1}^{M} \pi_{i+\Delta} X_i. \quad (7)$$

Considering the speed limitation of the robot or the possible locations of the robot in the next time step, only the positions within the access of the robot in the next time step are evaluated first. To maximize the decline of the uncertainties of the grid cells in the searching area, the robot should go to the position P with maximum fitness E_P. If all these positions around the robot have small E_P less than a given threshold η_E, then the range of candidate positions should be enlarged. When the range is enlarged up to the whole searching area and still the maximum fitness E_P is less than η_E, the MSOL mission can be finished and the robot should be stopped. In this study, η_E is chosen as 0.5.

4 Simulations and Results

4.1 Simulation Setup

In our research, in order to have a repeatable and controllable flow-field and plume, and also to reduce the computational load, a flow-field file with frame structure, just like a movie, is generated from the simulation platform released by Jay A. Farrell and his colleagues [21]. The file has a constant time interval 0.5s between consecutive frames, and each frame contains the flow information with

15×15 grids as well as the positions and concentrations of all odor puffs. All data in a frame was intercepted and saved during the running of the Farrell's simulation platform without any modification. In this research, the code of the simulation platform [21] was modified to have several odor sources. On our simulation experiment platform, the flow-field file is replayed, but almost without any calculation because the calculation has been done on the Farrell's platform when the file was being generated.

In this research, two exploratory behaviors were simulated and compared. One is to follow a predefined path shaped like rectangular wave in our most recent study [19], and the other is to search along the dynamic-planned route detailed in section 3. Both exploration methods worked side-by-side with the same odor-sources mapping algorithm using the D-S inference described in section 2. In the two simulations with different exploratory behaviors, the MOSL task, the environment and other conditions were set being same to have a fair comparison. The virtual robot can achieve a maximum speed of 0.5 m/s, the mean airflow velocity is about 1.0 m/s and the mean airflow direction is about 0°. There are two odor sources located at (20.0m, 50.0m) and (24.0m, 55.0m), respectively, with same area 0.3m×0.3m. The robot starts at the location (33.0m, 40.0m) to search a given rectangular region with left-top corner (18.7m, 60.3m) and right-bottom corner (32.7m, 40.3m). During the exploration, at each time step, the robot collects the odor concentration, airflow speed and direction by the equipped gas sensor and the anemometer, respectively.

4.2 Simulation with the Predefined Path

In our earlier work [19], the robot simply follows a predefined path shaped like rectangular wave to cover the given searching region, performing an exploratory behavior. It firstly goes to the right-bottom corner and then vertically up to the top bound of the given region, and then goes vertically down to the bottom bound with a fixed offset 2m in left direction, and so on. When the robot arrives at the left-top corner (called 1 round, see Fig. 1(a)), the robot comes back to the right-bottom corner, and starts a new round of the exploration, and so on. Figure 1 illustrates three scenes of the estimated distribution of the two odor sources, in which the work area of the robot is marked by a yellow rectangle.

The MOSL mission was aborted when the 5th round was complete. The mission spent 4283.5s and the robot travelled 1060.8m totally, and the sum of the uncertainties (defined in Equ. (5)) of all cells in the work area was 254.1.

It can be found from Fig. 1 that, the distribution map of the two odor sources was updated recursively via the D-S inference using new coming evidence from the successive measurements by the robot when the robot followed the predefined path in the given searching area. Apparently, the mapped locations of the two odor sources approached to the true sites as evidence accumulates.

It also can be found that in Fig. 1(c), near the right bound of the searching area, there were still some cells with unclear states although the robot has completed the 5th round exploration. This is because that, the mean airflow direction was about 0° in this simulation, and the robot often had detection events near the right bound, resulting some cells with confusing information. This result suggests that more exploration should be performed for these cells.

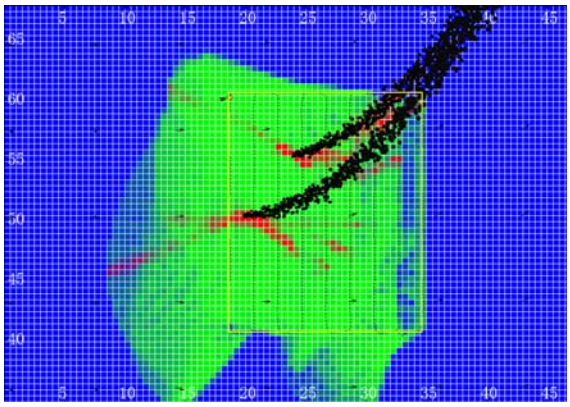

(a) 1st round, cost 781.5s and travelled 193.5m, leaving a sum of uncertainties of the cells in the searching area about 1089.0

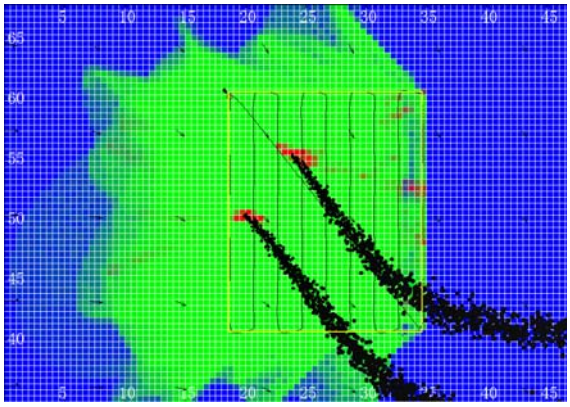

(b) 3rd round, cost 2532.5s and travelled 627.1m, leaving a sum of uncertainties of the cells in the searching area about 374.6

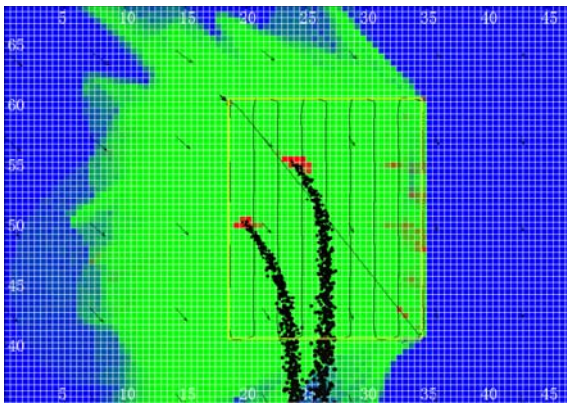

(c) 5th round, cost 4283.5s and travelled 1060.8m, leaving a sum of uncertainties of the cells in the searching area about 254.1

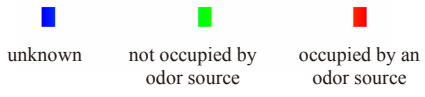

Fig. 1. Estimated distribution maps of two odor sources at different time using the D-S inference algorithm with a predefined searching path shaped like rectangular wave. The yellow rectangle marks the work area of the robot, with left-top corner (18.7m, 60.3m) and right-bottom corner (32.7m, 40.3m).

4.3 Simulation with the Dynamic-planned Searching Route

With the exploration algorithm proposed in this paper, the robot searches the work area in dynamic directions resulted from the current uncertainty map of the odor sources and the time-varying airflow information. Figure 2 illustrates three scenes of the estimated distribution of the two odor sources, in which the work area of the robot is marked by a yellow rectangle. The robot finished the MOSL mission using 2500.0s, and travelled 496.1m totally. The sum of the uncertainties of all cells in the work area was 157.1.

From Fig. 2, we can find that, using the D-S inference, the distribution map of the two odor sources was updated recursively as well as the one in Fig. 1. The robot searched the work area in a dynamic direction resulted from the current uncertainty map of the odor sources and the time-varying airflow information, leaving a wandering trajectory. As a result, the possible locations of the two odor sources can be estimated and marked as the evidence accumulates. In Fig. 2(c), several cells in the work area still had false information of being occupied by an odor source. The possible reason is the robot often had odor detections when the robot made exploration near these cells. In addition, it needs to point out that the cells outside of the searching area, including the states of them, should be ignored although they were marked. This is because the planning of the searching route never considered these cells but the estimation of they states were carried out incidentally with the D-S inference.

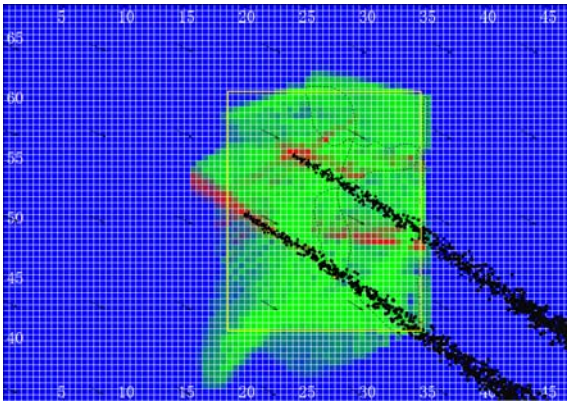

(a) 1st scene at 400.0s, travelled 97.4m, leaving a sum of uncertainties of the cells in the searching area about 1317.4

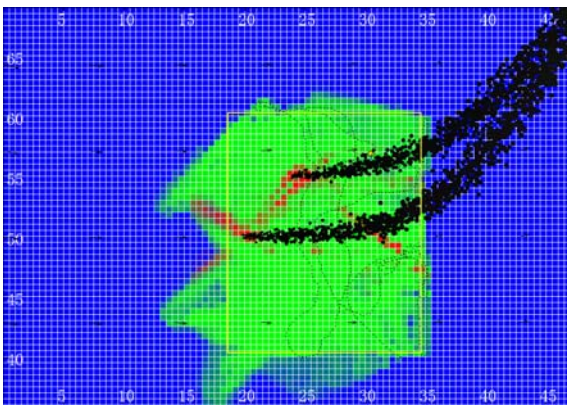

(b) 2nd scene at 800.0s, travelled 183.8m, leaving a sum of uncertainties of the cells in the searching area about 683.0

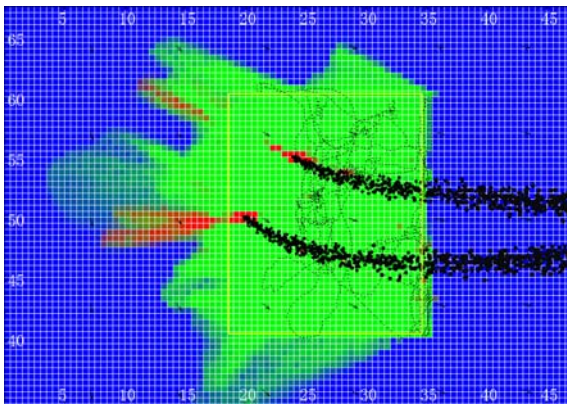

(c) 3rd scene at 2500.0s, travelled 496.1m, leaving a sum of uncertainties of the cells in the searching area about 157.1

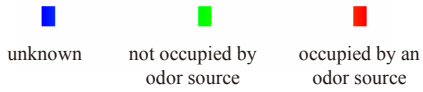

Fig. 2. Estimated distribution maps of two odor sources at different time using the D-S inference algorithm with the dynamic-planned searching route resulted from the current uncertainty map of the odor sources and the time-varying airflow information. The yellow rectangle marks the work area of the robot, with left-top corner (18.7m, 60.3m) and right-bottom corner (32.7m, 40.3m).

4.4 Comparison and Discussion

From the results of the two MOSL mission with different exploratory behaviors described in section 4.2 and 4.3, it is not hard to find that, both exploration method can be used to cover the searching area and work side-by-side with the D-S inference, and the locations of the multiple odor sources can be estimated online with the D-S inference. In comparison with the exploration following the predefined path, the exploration with dynamic-planned searching route cost much less time and had a shorter trajectory but made a clearer map.

Both in Fig. 1(c) and Fig. 2(c), i.e., when the MOSL missions were aborted, some cells still had unclear states. The common possible reason is the robot often had odor detection events when the robot made exploration near these cells. This problem suggests that some other methods should be considered next to declare the mapped “odor sources”, and thus can avoid the excessive exploration and limit the time cost.

5 Conclusion

In this research, the robot carries out the D-S inference and iteratively updates a grid map indicating the possible locations of the two odor sources, using the successive measurements from a gas sensor and an anemometer when the robot searches the given region in a dynamic direction resulted from the current uncertainty map of the odor sources and the time-varying airflow information. Simulations are carried out and the results in a time-varying airflow environment show that the locations of the multiple odor sources can be estimated online and approach to the true sites as the evidence accumulates. Compared with the exploration following a predefined path shaped like

rectangular wave, the exploration with dynamic-planned searching route cost much less time and had a shorter trajectory but made a clearer map. In addition, the simulation results suggest that some other methods should be considered next to declare the mapped "odor sources", and thus can avoid the excessive exploration and limit the time cost. The proposed MOSL method has a low computational cost, and can be used in online applications.

ACKNOWLEDGMENT

The authors would like to thank Professor J. A. Farrell from University of California, Riverside, U.S.A., for providing the source code for the advection–diffusion plume model.

References

[1] Sandini, G., G. Lucarini, and M. Varoli. Gradient driven self-organizing systems. in *Proceedings of International Conference on Intelligent Robots and Systems*. 1993. p.429-432.

[2] Consi, T.R., et al. AUV guidance with chemical signals. in *Proceedings of IEEE Sympsium on Autonomous Underwater Vehicle Technology*. 1994. p.450-455.

[3] Russell, A., D. Thiel, and A. Mackay Sim. Sensing odour trails for mobile robot navigation. in *Proceedings of IEEE International Conference on Robotics and Automation*. 1994. p.2672-2677.

[4] Ishida, H., et al. , Study of autonomous mobile sensing system for localization of odor source using gas sensors and anemometric sensors. *Sensors and Actuators A: Physical*, 1994. 45(2): p. 153-157.

[5] Lilienthal, A.J., A. Loutfi, and T. Duckett, Airborne chemical sensing with mobile robots. *Sensors*, 2006. 6(11): p. 1616-1678.

[6] Farrell, J.A., S. Pang, and W. Li, Chemical plume tracing via an autonomous underwater vehicle. *IEEE Journal of Oceanic Engineering*, 2005. 30(2): p. 428-442.

[7] Zarzhitsky, D., D.F. Spears, and W.M. Spears. Distributed robotics approach to chemical plume tracing. in *Proceedings of International Conference on Intelligent Robots and Systems*. 2005. p.4034- 4039.

[8] Berg, H.C. Bacterial microprocessing. in *Proceedings of Cold Springs Harbor Symp, Quantum Biology*. 1990. p.539–545.

[9] Belanger, J.H. and M.A. Willis, Adaptive control of odor-guided locomotion: behavioral flexibility as an antidote to environmental unpredictability. *Adaptive Behavior*, 1996. 4(3-4): p. 217-253.

[10] Vergassola, M., E. Villermaux, and B.I. Shraiman, 'Infotaxis' as a strategy for searching without gradients. *Nature*, 2007. 445(7126): p. 406-409.

[11] Li, W., et al. , Moth-inspired chemical plume tracing on an autonomous underwater vehicle. *IEEE Transactions on Robotics*, 2006. 22(2): p. 292-307.

[12] Kowadlo, G. and R.A. Russell, Using naïve physics for odor localization in a cluttered indoor environment. *Autonomous Robots*, 2006. 20(3): p. 215-230.

[13] Kowadlo, G. and R.A. Russell, Improving the robustness of naive physics airflow mapping, using Bayesian reasoning on a multiple hypothesis tree. *Robotics and Autonomous Systems*, 2009. 57(6-7): p. 723-737.

[14] Ishida, H., T. Nakamoto, and T. Moriizumi, Remote sensing of gas/odor source location and concentration distribution using mobile system. *Sensors and Actuators B: Chemical*, 1998. 49(1-2): p. 52-57.

[15] Lilienthal, A. and T. Duckett, Building gas concentration gridmaps with a mobile robot. *Robotics and Autonomous Systems*, 2004. 48(1): p. 3-16.

[16] Pang, S. and J.A. Farrell, Chemical plume source localization. *IEEE Transactions on Systems, Man and Cybernetics, Part B (Cybernetics)*, 2006. 36(5): p. 1068-1080.

[17] Ferri, G., et al. , Mapping multiple gas/odor sources in an uncontrolled indoor environment using a Bayesian occupancy grid mapping based method. *Robotics and Autonomous Systems*, 2011. 11(59): p. 988–1000.

[18] Li, J.G., et al. , Odor source localization using a mobile robot in outdoor airflow environments with a particle filter algorithm. *Autonomous Robots*, 2011. 30(3): p. 281-292.

[19] Li, J., et al. Odor sources mapping with D-S inference in time variant airflow environments via a mobile robot. in *IEEE International Conference on Cyber Technology in Automation, Control and Intelligent Systems*. 2015. in press.

[20] Shafer, G., *A Mathematical Theory of Evidence*. 1976, Princeton: Princeton University Press.

[21] Farrell, J.A., et al. , Filament-based atmospheric dispersion model to achieve short time-scale structure of odor plumes. *Environmental Fluid Mechanics*, 2002. 2(1): p. 143-169.